Secondary-Structure Characterization of Two Proficient Kinase Deoxyribozymes†

John C. Achenbach, Greg A. Jeffries, Simon A. McManus, Lieven P. Billen, and Yingfu Li*

Department of Biochemistry and Biomedical Sciences and Department of Chemistry, McMaster University, 1200 Main Street West, Hamilton, Canada

Received August 6, 2004; Revised Manuscript Received January 3, 2005

ABSTRACT: Dk1 and Dk2 are two catalytically proficient, manganese-dependent, guanine-rich deoxyribozymes previously isolated for DNA phosphorylation. In this study, we carried out a series of experiments that aimed to understand the structural properties of Dk1 and Dk2 and compare the structural similarities or differences of these two distinct deoxyribozymes that carry out similar catalytic functions. First, we performed reselections from two partially randomized DNA libraries on the basis of the original Dk1 and Dk2 sequences to isolate catalytically active sequence variants and identify nucleotides that are invariable, well-conserved, or highly mutagenized. Sequence analysis of these variants assisted by secondary-structure predictions led to the identification of possible Watson−Crick base-pairing regions within each deoxyribozyme. Sequence truncation and base-pair partner exchange experiments were conducted to confirm, or rule out, the existence of the predicted secondary-structure elements. Finally, methylation interference experiments were applied to identify nucleotides that are potentially important for the tertiary structure folding of the deoxyribozymes. Our data suggest that Dk1 and Dk2, despite the differences in their primary sequences and NTP requirements, use an analogous stem-loop element to anchor a structural domain of substantial tertiary interactions to execute their catalytic functions.

In the past 10 years, intensive studies have demonstrated that, like their natural and artificial RNA counterparts, catalytic DNA (also referred to as deoxyribozymes or DNAzymes) has the ability to catalyze a plethora of chemical reactions on a biologically relevant time scale. Many studies have centered on the isolation of activities that mimic those of natural protein enzymes such as RNA cleavage (*1*−*10*), DNA cleavage (*11, 12*), DNA phosphorylation (*13, 14*), DNA adenylation (*15*), DNA ligation (*16*−*18*), RNA ligation (*19, 20*), *N*-glycosylase activity (*21*), and porphyrin metalation (*22*). Some of the isolated DNAzymes can achieve rate enhancements of up to 10^{10} fold (*15*). Recently, DNA has been used as the medium to create catalytic molecules with practical applications such as fluorescence signaling (*23*−*27*) and RNA manipulation (*28*).

As the list of chemical transformations catalyzed by DNA expands and its application in the field of biotechnology broadens, it becomes increasingly pertinent to study the means by which this polymer, once thought to be catalytically "unfit", performs catalysis up to 10^{10} times faster than the uncatalyzed reaction (*15, 29*). Understanding a DNAzyme's secondary, and ultimately tertiary, structure is a key step in this process. This type of study is exemplified by the recent crystallographic work in the analogous field of ribozymes (*30*−*32*).

Our lab recently used DNA phosphorylation (Figure 1A) as a model system to study the ability of divalent metal ions to support DNA-mediated catalysis. The use of several divalent metal ions during parallel in vitro selection experiments led to the creation of catalytic pools of metallo-DNAzymes with incredible sequence diversity. Dk1[1] and Dk2, the two dominant Mn^{2+}-dependent DNAzymes identified in this study, are both proficient with k_{cat}'s of 2.8 and 0.8 min^{-1}, respectively, under optimized conditions (*14*). However, they differ in their substrate specificities. Dk1 selectively uses ATP with a K_M of 0.85 mM, while Dk2 requires GTP with a K_M of 0.55 mM (*14*). Their impressive catalytic rate enhancements (10^9-fold over the spontaneous hydrolysis of ATP) and selective use of divalent metal ion cofactors make Dk1 and Dk2 excellent model systems for studying metal-promoted DNA-mediated catalysis. Perhaps the most intriguing aspect of these metallo-DNAzymes is their similarity in divalent metal ion requirements and catalytic rates despite the differences in primary sequence and substrate specificity. It is hoped that further characterization of these two self-phosphorylating DNAzymes could reveal important structural information and help determine what structural strategies they use to solve the same catalytic "question".

In this study, we sought to further characterize the secondary structures of these two self-phosphorylating deoxyribozymes. A reselection experiment was performed to identify the nucleotides in Dk1 and Dk2 that are essential for catalysis. Both deoxyribozymes were truncated to reveal

† This work was supported by research grants from the Canadian Institutes of Health Research, Natural Sciences Research Council of Canada (NSERC), and Canada Foundation for Innovation. JCA and LPB are both recipients of NSERC postgraduate scholarships. YL is a Canada Research Chair.

* To whom correspondence should be addressed. E-mail: liying@mcmaster.ca; tel: (905) 525−9140; fax: (905) 522-9033.

[1] Abbreviations: ATP, adenosine 5′-triphosphate; CIAP, calf-intestine alkaline phosphatase; Dk1, deoxyribozyme kinase 1; Dk2, deoxyribozyme kinase 2; DMS, dimethyl sulfate; DTT, dithiothreitol; EDTA, ethylenediamine tetraacetic acid; GTP, guanosine 5′-triphosphate; NTP, nucleoside 5′-triphosphate; PAGE, polyacrylamide gel electrophoresis; PCR, polymerase chain reaction; T4 PNK, T4 polynucleotide kinase.

10.1021/bi0483054 CCC: $30.25
Published on Web 02/18/2005

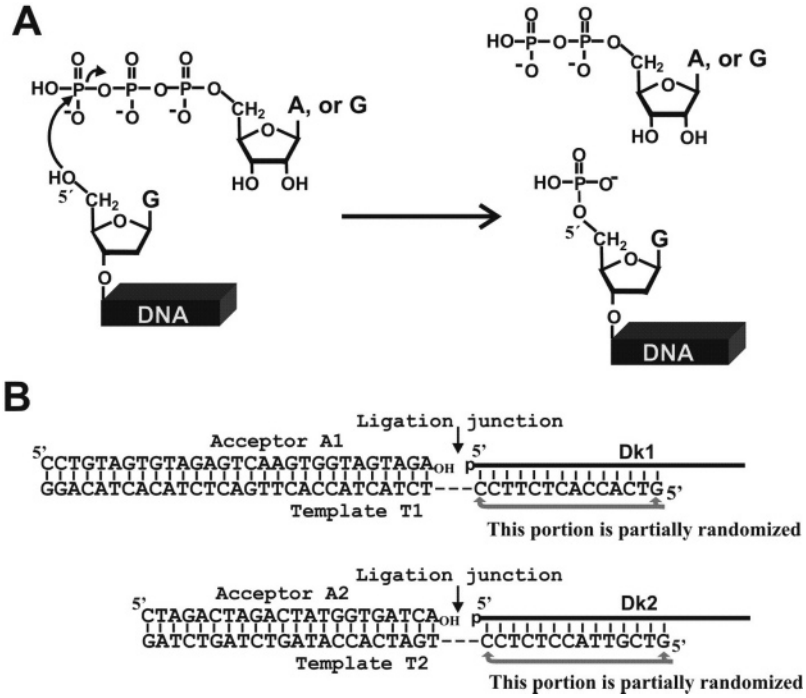

FIGURE 1: (A) General reaction scheme for self-phosphorylating deoxyribozymes. (B) Sequences of acceptor and template oligonucleotides used in reselections and enzymatic assays. A portion of the templates used for reselections was partially randomized (24% mutation rate) to accommodate the partial randomization of the libraries.

minimal catalytically essential sequences that are substantially shorter than those isolated from in vitro selection. Secondary-structure predictions were examined through mutational analysis to reveal a common structural theme exhibited by both Dk1 and Dk2: a stem-loop element flanked by two highly conserved and catalytically relevant arms within which numerous guanine residues were implicated in potential tertiary interactions through methylation interference experiments.

MATERIALS AND METHODS

Oligonucleotides and Materials. Synthetic DNAs were prepared by automated chemical synthesis (HHMI-Keck Biotechnology Resource Laboratory, Yale University; Central Facility, McMaster University; Alpha DNA, Montreal; Sigma Genosys, Oakville, Ontario). The partially mutagenized variant libraries used for reselection were synthesized using the following mixture of the four standard phosphoramidates: 76% of the wild-type nucleotide, 8% of each of the remaining three nucleotides. DNA oligonucleotides were purified by 10% denaturing (8 M urea) PAGE. Purified oligonucleotides were dissolved in water and their concentrations were determined spectroscopically. [γ-^{32}P]ATP, [α-^{32}P]-dATP, and [α-^{32}P]dGTP were purchased from Amersham Pharmacia. Nucleoside 5′-triphosphates, T4 DNA ligase, T4 polynucleotide kinase (PNK), calf-intestine alkaline phosphatase (CIAP), and M-MuLV reverse transcriptase were purchased from MBI Fermentas. All other chemical reagents were purchased from Sigma.

Dk1 and Dk2 Variant Reselection Procedures. The basic protocol for both the Dk1 and Dk2 variant reselections is similar to the one used by Wang et al. (*14*) with the following specifics. One thousand picomoles of the partially randomized DNA library was used as the initial pool (G0). DNA was heated to 90 °C for 2 min and cooled to room temperature. A 2× selection buffer [100 mM HEPES (pH 7.0 at 23 °C), 800 mM NaCl, 200 mM KCl, 20 mM $MnCl_2$] was then added to the reaction mixture and left to incubate for 5 min. ATP or GTP (final concentration: 1 mM) was added to initiate the Dk1 and Dk2 phosphorylation reactions, respectively. The reaction mixture for the first round of selection contained 0.5 μM DNA.

The DNA mixture was incubated for self-phosphorylation at 23 °C for 10 min. The phosphorylation reaction was stopped by the addition of EDTA (pH 8.0) to a final concentration of 30 mM. DNA was recovered by precipitation with ethanol, resuspended in T4 DNA ligase buffer (40 mM Tris-HCl pH 7.8 at 25 °C, 10 mM DTT), and supplied with 2000 pmol of partially randomized template DNA and 2500 pmol of acceptor DNA (A1 or A2; Figure 1B). The mixture was heated to 90 °C for 1 min and cooled to room temperature over 2 h to promote proper template annealing. ATP (final concentration 0.5 mM) and T4 DNA ligase (0.01 u/μL, final concentration) were then added to start the ligation reaction. The solution was incubated at 23 °C for 1 h before the DNA was recovered by precipitation with ethanol.

Ligated DNA was separated from unligated DNA by denaturing 10% PAGE following a procedure described in detail by Li and Breaker (*13*). The 123-nt ligated DNA product was amplified by PCR. Double-stranded DNA was recovered by precipitation with ethanol, resuspended in 90 μL of 0.25 M NaOH, and incubated at 90 °C for 10 min to cleave the single-embedded RNA linkage. The ~100-nt DNA cleavage fragments, corresponding in length to the original DNA constructs, were purified by denaturing 10% PAGE. Finally, alkaline phosphatase was used to treat the purified 100-nt DNA to remove potential 5′-phosphate group so as to prevent the appearance of certain "selfish", noncatalytic DNAs that can obtain a 5′-phosphate during the PCR reaction (*13*).

Three additional rounds of selection were performed as described above except the total amount of DNA was reduced to 25 pmol. The G4 populations from both reselections were then cloned and sequenced.

Cloning and Sequencing of DNA Populations. DNA sequences from a relevant selection round were amplified by PCR and cloned into a pUC57 derivative using the T/A cloning method. Plasmids containing individual catalysts were isolated and purified using the 96-well PerfectPrep kit (Eppendorf). Inserts were unidirectionally sequenced with the −47 primer on a CEQ 2000XL DNA sequencer (Beckman-Coulter) using the CEQ Quick Start Kit (Beckman-Coulter) as directed by the manufacturer.

Catalytic Assays. DNAzyme constructs used in secondary-structure assays were constructed from the ligation of two oligonucleotides with donor oligonucleotides labeled at their 5′-end with ^{32}P. Thus, all DNAzyme constructs were internally ^{32}P-labeled. Ligation was performed as follows. Fifty picomoles of donor DNA was phosphorylated in the presence of [γ-^{32}P]ATP at a final DNA concentration of 1 μM. Unlabeled ATP (final concentration 3.8 mM) was then added to the reaction mixture and incubated for a further 30 min to ensure full phosphorylation. After a 5-min incubation at 90 °C to inactivate the PNK, the phosphorylation reaction mixture was added directly to a ligation reaction mixture containing 75 pmol template and 90 pmol acceptor DNA (total DNA concentration 1 μM). Ligation proceeded for 1 h at 23 °C, followed by ethanol precipitation. Ligated product was isolated by denaturing 10% PAGE.

Constructs used in methylation interference experiments (see below) and "substrates" for trans reactions were 3′-labeled using a primer extension protocol containing [α-^{32}P]-dATP or [α-^{32}P]dGTP. Briefly, 50 pmol of the deoxyribozyme construct or a trans substrate missing the 3′-terminal nucleotide was heated to 90 °C with 60 pmol of a template with a 1-nt 5′-overhang. The mixture was cooled to room temperature and the reaction buffer (supplied with the enzyme), along with the radiolabeled nucleotides, was added, followed by 200 units of M-MuLV reverse transcriptase (MBI Fermentas). Labeled deoxyribozyme constructs were PAGE-purified.

All deoxyribozyme constructs were CIAP-treated as follows to remove any 5′-phosphate. DNA (final concentration 2 μM) was heated to 90 °C in the absence of buffer salts and cooled quickly to room temperature to prevent structural folding. CIAP buffer and three units of CIAP were added and the reaction mixture was incubated for 1 h at 37 °C. DNA was purified through two successive phenol-chloroform extractions.

DNAzyme constructs were tested for the ability to self-phosphorylate using the same indirect ligation method used in the variant reselection. For self-phosphorylation of cis constructs, reaction volumes were typically 10 μL with a total DNAzyme concentration of 0.1 μM. Each DNAzyme construct was refolded by heating to 90 °C in water for 5 min and cooled to room temperature over 10 min. The 2× selection buffer was then added, followed by an additional 5-min incubation at room temperature. The reactions were initiated by adding 1 mM of either ATP or GTP to the Dk1 or Dk2 solutions, respectively. A solution containing 15 mM Na_2EDTA (final concentration), 10 pmol of template, and 15 pmol of acceptor (see Figure 1B) was added to quench the reaction. This was immediately followed by 2.5 volumes of cold ethanol for precipitation. Following two 70% ethanol washes, the mixture of the DNAzyme, template, and acceptor DNA was resuspended in 26 μL of water, heated to 90 °C for several minutes, and cooled to room temperature over 10 min to promote proper annealing. Three microliters of 10× ligase buffer (MBI-Fermentas) and five units of T4 DNA ligase were added to initiate the ligation reaction, which was allowed to proceed at room temperature for 1 h. DNA was recovered by ethanol precipitation and the ligated product was resolved by 10% denaturing PAGE. Bimolecular reactions of trans constructs were performed in the same manner with "enzyme" and "substrate" concentrations of 1 μM and 0.1 μM, respectively.

The rate constants for DNA phosphorylation were determined by plotting the natural logarithm of the fraction of DNA that remains unligated versus the reaction time. The negative slope of the line produced by a least-squares fit to the data was taken as the rate constant. All specified rates in the text and in Supplementary Figure 2 are the average of at least two independent time-course experiments.

Methylation Interference Assays. A solution of 0.2 μM 3′-labeled DNA (5 pmol) in water was heated to 90 °C for 1 min and cooled to room temperature quickly to disrupt folding. The methylation reaction was initiated by adding an equal volume of 0.04% (v/v) DMS (freshly made), followed by incubation at room temperature for 40 min. Methylated DNA was recovered by ethanol precipitation, followed by two washes in 70% ethanol. Self-phosphorylation reactions using the same conditions as described for the reselection experiments were performed as described above (total DNAzyme concentration: 0.1 μM; incubation time: 1 min). For control samples, the self-phosphorylation reaction was carried out before the methylation reaction. For both sets of reactions, catalytically active molecules were separated from inactive using the ligation assay described above. Ligated bands were isolated, eluted from the gel, recovered through ethanol precipitation, and subjected to methylation-dependent cleavage in 50 μL 10% (v/v) piperidine for 30 min at 90 °C. The resultant cleavage products were dried under vacuum and analyzed by 10% denaturing PAGE.

Densitometry on bands from both the test and control lanes was performed to score the degree of methylation interference observed. The difference in background-corrected band intensity between equivalent cleavage fragments from each lane was normalized using the difference observed in a pair of cleavage fragments originating from a guanine located in the confirmed catalytically unimportant stem-loop region of each construct. The ratio of intensities for each pair of bands (R) was determined by dividing the corrected band intensity in lane T (test lane) by the corrected band intensity from lane C (control lane). These ratios were then normalized on a scale from 0 to 100, where 0 indicates the least interference and 100 the most, using the following equation: $R_{\text{normalized}} = [(R - R_0)/(R_{100} - R_0)] \times 100$. In their respective experiments, R_0 and R_{100} were the ratios of the band pairs corresponding to G33 and G21 of Dk1 and G24 and G2 of Dk2.

RESULTS

Dk1 and Dk2 Reselections. Our first objective was to identify the nucleotides in Dk1 and Dk2 that are essential

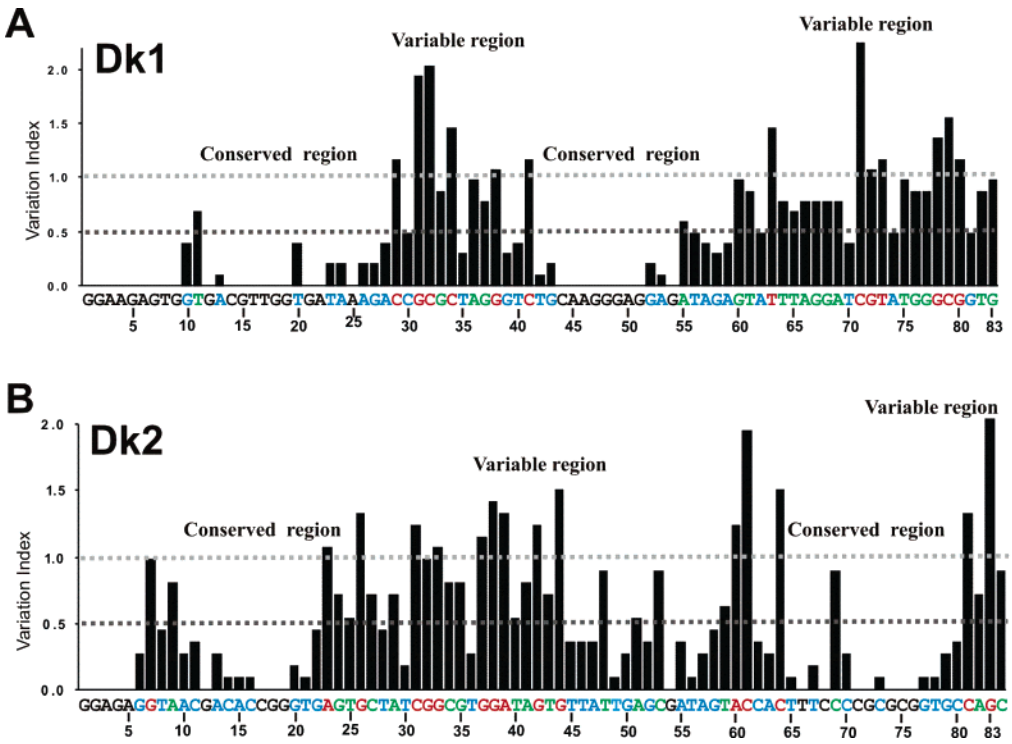

FIGURE 2: Sequence analysis of terminal pools from reselection. ~40 clones were sequenced from the terminal population of the Dk1 reselection (A) and the Dk2 reselection (B). The variation index was calculated by dividing the observed mutation rate at each position by 24% (the mutation rate of the starting library). The wild-type sequence is shown at the bottom of each chart (the 3′ constant region is omitted). Nucleotides are colored in the following manner: black, absolutely conserved; blue, variation index between 0 and 0.5; green, variation index between 0.5 and 1; red, variation index >1 (this coloring scheme is used in all subsequent figures as well).

for catalysis. A reselection experiment was performed starting with chemically synthesized, partially mutagenized libraries on the basis of the Dk1 and Dk2 sequences. These libraries were synthesized with a 24% mutation rate at every nucleotide position except the 15-nt primer-binding region on the 3′-end following a previous protocol (*13*).

The in vitro selection scheme was identical to that used in the primary isolation of these DNAzymes (*14*). The in vitro selection scheme relies on the ligation of an acceptor molecule to molecules that have successfully phosphorylated their 5′-hydroxyl groups to provide a means of selection and subsequent PCR amplification (*13*). To prevent cross-contamination between two Dk populations and hijacking of the reselections by Dk1 and Dk2 molecules leftover from the original selection, new and unique template and acceptor pairs (T1 and A1, T2 and A2; Figure 1B) were employed in the current study. The portion of the templates that anneals with the 5′ end of the library was also partially randomized at a 24% mutation rate. In doing so, we hoped to accommodate the partial randomization at the 5′-end of each deoxyribozyme during the ligation step and thus relax the restriction on the sequence requirement at the 5′ end of the deoxyribozymes compared to where a single template sequence is used. This relaxation is made possible by the fact that T4 DNA ligase accommodates mismatches at or near the ligation junction (*33*). In addition, we intentionally employed long annealing and ligation times to reduce the number of inevitable mismatches between the mixed-sequence template and partially randomized library for each reselection.

One thousand picomoles of each library was allowed to react with either ATP (Dk1 reselection) or GTP (Dk2 reselection) in the presence of 1× selection buffer (50 mM HEPES pH 7.0, 400 mM NaCl, 100 mM KCl, 10 mM $MnCl_2$) (*14*). To identify mutations that have no significant effect on the rate of catalysis, incubation times during the self-phosphorylation step were kept short at 10 min throughout the reselection. After four rounds of selective amplification, both Dk1 and Dk2 populations reached ~20% reaction completion and were cloned and sequenced.

Forty-two and 46 clones were sequenced from the cloned Dk1 and Dk2 pools, respectively. On average, each sequence acquired approximately 10 mutations as compared to the original Dk1 and Dk2 sequences. There were no identical sequences found. The sequences of all isolated clones are given in Supplementary Figure 1 and a statistical analysis of the data is shown in Figure 2, where the original sequences of Dk1 (Figure 2A) and Dk2 (Figure 2B) are shown with the variation index (a measure of variability) plotted for each base position. The variation index was calculated by dividing the observed mutation rate at each position by 24%, which is the mutation rate of the starting library. A variation index of 0 indicates that the base is absolutely conserved in all the sequenced clones and these bases are colored black. In theory, if there are no constrictions on a base position, the variability observed within the sequenced population should be equivalent to the mutation rate (i.e., 24%); in such cases, the variation index would be 1. Values greater than 1 could indicate that mutations confer a selective advantage over the original base. These bases are indicated in red. By far the majority of positions from both reselections have variation indices between 0 and 1. We arbitrarily chose values of below 0.5 to indicate partial conservation (indicated in blue). Bases with values above 0.5 but below 1 are colored in green.

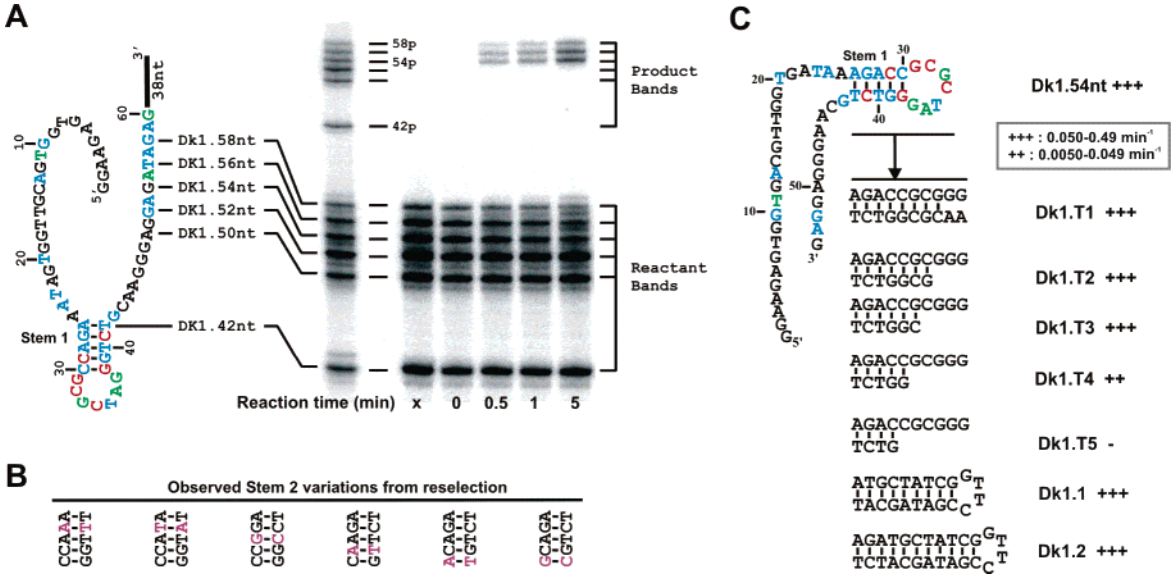

FIGURE 3: Secondary structure of Dk1. (A) Sequence truncation. A predicted Dk1 secondary structure is shown, along with a gel-based parallel time course of several Dk1 3′ truncation mutants. The location of substrate bands and the corresponding product bands of the 58, 54, and 42-nt truncation mutants are indicated. "x" indicates a negative control where no ATP was added to the reaction. Only the 54, 56, and 58-nt deletion mutants appear to be active. (B) Base-pair covariation patterns observed in the Dk1 mutants from the reselection. The altered base pairs are highlighted in purple. (C) Examination of the predicted stem in Dk1. The truncated version of Dk1 was separated into "enzyme" and "substrate" portions that could associate through several Watson−Crick base pairs. Deoxyribozyme constructs with a stem containing 4−8 bp are examined for catalytic activity. In addition, two new constructs with significantly altered base pairs in the stem were also tested for self-phosphorylating capability.

This coloring scheme is maintained in all remaining figures. The 15-nt 3′-primer-binding sequences of both deoxyribozymes are omitted in Figure 2 for simplicity. Their conservation is required for amplification during the reselection process, and thus they remained invariable.

Interestingly, both Dk1 and Dk2 exhibited similar overall patterns of conservation. Each deoxyribozyme contained a center of high variability surrounded by regions with reduced variability. Each of them also had a highly variable 3′ end and a highly conserved 5′ end.

Secondary Structure of Dk1. The predicted secondary structure for Dk1 (Figure 3A) by the M-fold program (*34*) correlates with the observed variability data. The central variable region clusters in the location of the putative stem and 7-nt loop. Interestingly, the G-rich conserved regions flanking this stem-loop appear to have no predictable secondary structure.

We tested six different 3′-truncated constructs (from 58 to 42 nucleotides in length, see Figure 3A) in an effort to isolate the minimal essential catalytic sequence. All six were tested together in the selection buffer containing 1 mM ATP. Figure 3A shows a representative gel from a time-course experiment. The Dk1 constructs shorter than 54 nt were not active, as indicated by the absence of product bands. The smallest active construct (54 nt) also exhibited the highest activity with a k_{obs} of 0.3 min^{-1}. This shows that 44 nucleotides at the 3′ end of the original construct can be removed with little influence on the catalytic activity.

The existence of Stem-1 in Dk1 is strongly supported by the seven covarying base-paring patterns observed with the selected Dk1 mutants (the data are summarized in Figure 3B). In addition, a stem in a deoxyribozyme (as well a ribozyme) can often be used as the site for breaking a cis-acting system into a trans-acting construct. The putative 5-bp stem of Dk1 seemed a logical location for separating the deoxyribozyme into substrate and enzyme strands allowing for the phosphorylation reaction to occur in trans. Under single turnover conditions (10 enzymes:1 substrate), the bipartite version of the shortened Dk1 (with an addition of 5 bp for a toal of 10 bp), named "Dk1.T1" (Figure 3C, T denotes trans-acting), was indeed catalytically active with a k_{obs} of ~0.6 min^{-1}.

The high variability observed in the Dk1 variants in the putative stem (Figure 2A) suggests that this stem may simply serve a structural role. To further investigate the idea, we examined several trans constructs containing shortened stems (Figure 3C). Reduction of the stem length to 7 bp (Dk1.T2) and 6 bp (Dk1.T3) did not decrease the catalytic activity; further reducing the stem to 5 bp (Dk1.T4) caused a 10-fold activity decrease. The construct with only 4 bp (Dk1.T5) became inactive.

To unequivocally verify the noncatalytic role of the stem-loop, two chimeric Dk1 constructs were created in which the stem-loop of Dk1 was replaced with the stem-loop seen in Dk2 (the secondary structure of Dk2 will be discussed below). In the first construct (Dk1.1), the original Dk1 stem-loop after the initial A−T base pair was replaced with the stem-loop from Dk2. The second chimeric Dk1 constructed (Dk1.2) was more conservative as it maintained the first three base pairs of its original Dk1 stem-loop. Both of the Dk1 chimeras were active with observed rates similar to the parental Dk1 construct, indicating that the sequence content of the original stem-loop in Dk1 was irrelevant for catalysis.

Secondary Structure of Dk2. Similar to Dk1, the predicted secondary structure of Dk2 correlates with the variability data obtained through the reselection experiment (Figure 2B). Most of the variability observed in the reselection progeny clusters in a single stem-loop element (blue, green, and red bases in Figure 4). Replacement of the 20-nt putative loop with a tetraloop (Dk2.1 see Figure 4; the nucleotides of the

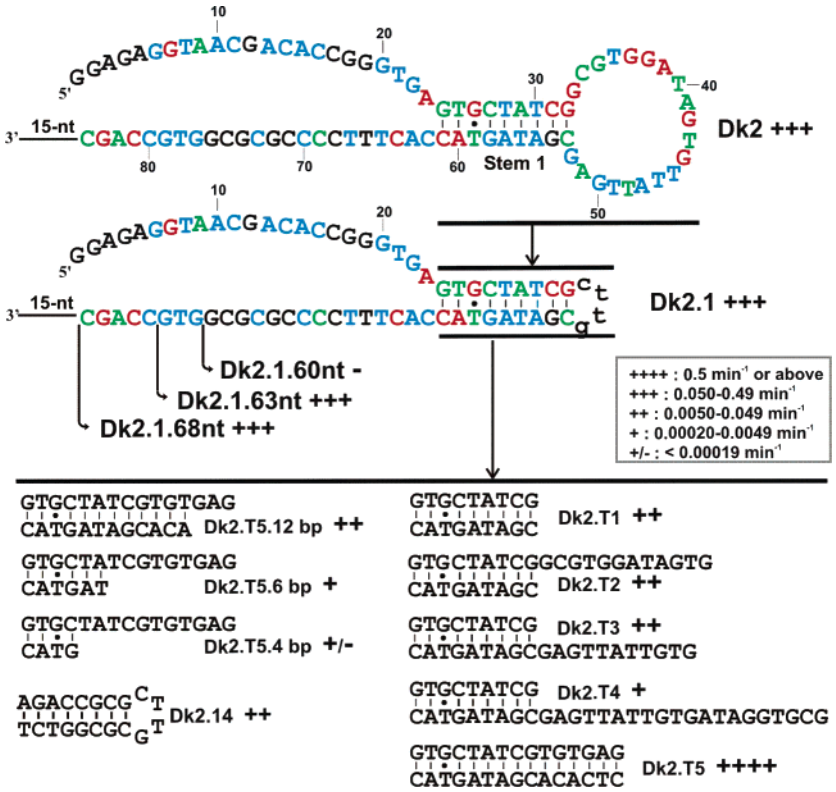

FIGURE 4: Secondary structure of Dk2: Part I. Many different deoxyribozymes are examined for the following purposes: (1) essentiality of the large loop (Dk.2.1), (2) truncation of unnecessary nucleotides at the 3′ end of Dk2 (Dk.2.1.60nt, Dk2.1.63nt, Dk2.1.68nt), (3) design of functional trans constructs (Dk2.T1, Dk2.T2, Dk2.T3, Dk2.T4, Dk2.T5, Dk2.T5.12bp, Dk2.T5.6bp, Dk2.T5.4bp), and (4) sequence dependence of Stem-1 (Dk.2.14). The artificial CTTG tetraloop is shown in lowercase letters.

tetraloop are shown in lowercase) resulted in only a modest reduction in rate, from 0.43 min^{-1} to 0.18 min^{-1} (all rates are listed in Supplementary Table 1). Further truncation of the 3′-conserved primer-binding site and five additional bases had no negative effect on deoxyribozyme activity. However, a further three-base truncation (Dk2.1.60nt in Figure 4) of some well-conserved bases inactivated the deoxyribozyme.

The putative Stem-1 in Dk2 also provided an opportunity to transform the DNAzyme into a trans-acting system with substrate and enzyme strands. Several trans constructs were constructed and all were active when tested under single-turnover conditions (1 substrate:10 deoxyribozymes). Removal of the loop region but maintenance of the 9-bp duplex (construct Dk2.T1 in Figure 4) resulted in an active deoxyribozyme with an approximate 7-fold reduction in the observed rate (0.04 min^{-1}) as compared to the corresponding cis construct Dk2.1.68nt (0.26 min^{-1}). To test whether the original 20-nt loop sequence affected enzymatic activity, trans constructs containing the 5′-portion of the loop (Dk2.T2), the 3′-portion of the loop (Dk2.T3), and the entire loop sequence (Dk2.T4) were assayed. None of these portions from the original sequence of the loop had any substantial effect on the observed rate. However, extension of the putative stem from 8 bp to 15 bp (Dk2.T5) increased the observed rate to a value that was 10-fold better than the cis construct.

The ability to create a trans version of Dk2 lends some support to the presence of the putative stem. However, as with Dk1, we decided to test whether the stability of the putative stem was responsible for the association of the two strands. The length of the enzyme portion, and thus the putative stem, was sequentially reduced from 15 bp (Dk2.T5) to a trans construct with only four possible base pairs. As expected, the observed first-order rates under single-turnover conditions decreased with the shortening of the putative stem (Figure 4). This demonstrates that, as observed for the trans version of Dk1, the stem interaction was again an essential component of the active structure of Dk2. We also produced a new cis-acting Dk2 construct (Dk2.14; Figure 4) in which Stem-1 was replaced with a stem equivalent to the 8-bp stem of the initial trans Dk1 construct ending with a tetraloop. Its catalytic activity did not differ from the parental Dk2.1 construct demonstrating that like the stem-loop in Dk1, the sequence of the stem-loop in Dk2 had no relevance to catalysis.

Three more Stem-1 variants were also tested and data are given in Figure 5. Replacing T44 with a C to remove the G−T wobble (Dk2.11) had no effect on enzymatic activity. The construct with an inverted C31-G38 base-pair (Dk2.12) resulted in a slightly increased catalytic rate. The third construct (Dk2.13) that contains both an inverted C31-G38 pair and a G26-C44 pair also exhibited a slightly enhanced activity.

Additional Stem Elements in Dk2. Unlike Dk1 which seems to lack substantial secondary structure other than the stem-loop, there are three smaller putative stems that can be predicted in the truncated version of Dk2 (Dk2.1.68nt), in addition to the stem-loop described above (as seen in Figure 5). To test the validity of these stem interactions, mutant constructs with flipped base pairs in these stems (lowercase and purple lettering in Figure 5) were assayed for catalytic activity.

All Stem-3 variants tested were inactive. Replacing T50 with a C abolished activity (Dk2.2). Inverting the putative

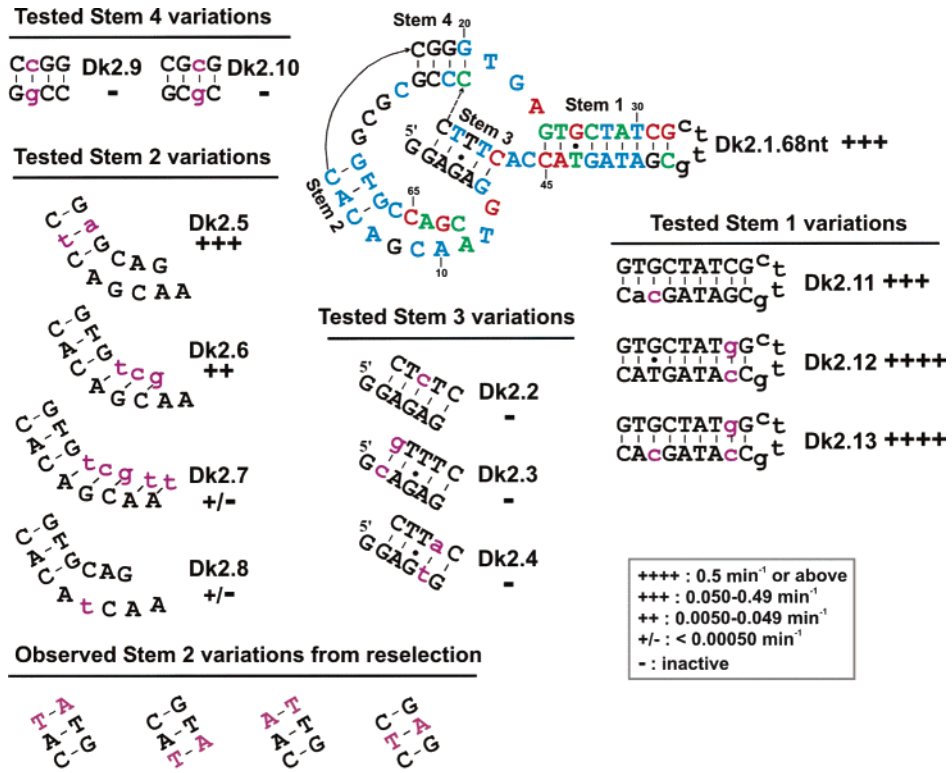

FIGURE 5: Secondary structure of Dk2: Part II. A total of four putative stems were identified and analyzed using complementary mutation experiments. The nucleotides of Dk2 modified for each test are highlighted in purple and shown in lowercase letters.

base pairs between G2-C52 (Dk2.3) and A5-T49 (Dk2.4) also inactivated the deoxyribozyme. This is not surprising as in all three cases the varied nucleotide positions were highly or absolutely conserved from the reselection experiment (Figure 2B). The two Stem-4 variants (Dk2.9 and Dk2.10) tested were also inactive. As with the Stem-3 variants, most nucleotide positions in this putative stem are absolutely conserved. The inability to identify sequence variation does not disprove the existence of such a stem. It may simply indicate that the sequence of the stem is also involved in some critical aspect of catalysis such as the formation of tertiary structure.

The existence of Stem-2 was consistent with the truncation experiments (Figure 4), which showed that removal of the three bases on the 3′-side of the duplex inactivated the deoxyribozyme. Sequence analysis of the selected Dk2 variants also revealed compensatory mutations consistent with Stem 2 (the compensatory mutations are also summarized in the bottom of Figure 5). The validity of Stem 2 was further tested by flipping of the A15-T62 base pair (Dk2.5). As seen in Figure 5, this change did not significantly alter enzymatic activity. Because Stem 2 is so small (3 bp), we wanted to see if lengthening this duplex would promote catalytic activity. Deoxyribozyme constructs with Stem 2 increased to six base pairs were indeed active (Dk2.6). However, extension of Stem 2 to eight base pairs resulted in loss of activity (Dk2.7). The observed effects may have resulted from an alteration of the proper secondary structural folding of the deoxyribozyme by the extended Stem 2. G12, a position seen to be absolutely conserved in this portion of the deoxyribozyme, was replaced with a T to confirm its essentiality. The mutant construct (Dk2.8) was barely active with an estimated k_{obs} of 1.1×10^{-4} min^{-1} demonstrating the importance of G12 for proper catalytic function.

Chemical Probing of Dk1 and Dk2 Using Dimethyl Sulfate. There are many conserved guanines within the seemingly unstructured region of Dk1. With very little evidence for secondary structure within Dk1, methylation interference experiments were performed to probe for possible involvement of these guanines in tertiary interactions. Although Dk2 contained several putative stem regions, the inability to confirm most of them hinted that perhaps Dk2 also contained extensive tertiary, noncanonical Watson−Crick interactions. It too was examined using the methylation interference approach. Methylation interference is a powerful and specific approach to indicate non-Watson−Crick interactions of guanines. Because the methylating agent dimethyl sulfate (DMS) preferentially methylates the N7 position of guanine, loss of catalytic activity upon methylation can indicate involvement in non-Watson−Crick hydrogen bond formation. Active constructs were isolated on the basis of their ability to ligate with an acceptor molecule and were chemically cleaved specifically at their methylated guanine using piperidine. Methylation may also disrupt tertiary folding that imparts steric constraints on the N7 position.

Radioisotopically labeled constructs (Figure 6) were partially methylated using DMS so that on average one guanine per molecule was methylated. The methylated deoxyribozyme constructs were then allowed to self-phosphorylate. Active constructs were isolated and were chemically cleaved specifically at their methylated guanine using piperidine. Cytosine and adenosine may also be methylated at N3 and N1, respectively; however, DNA molecules containing methylated cytosine and adenine usually are not prone to piperidine-mediated cleavage.

This type of assay required the use of end-labeled DNAzymes. The catalytic activity of the DNAzymes pre-

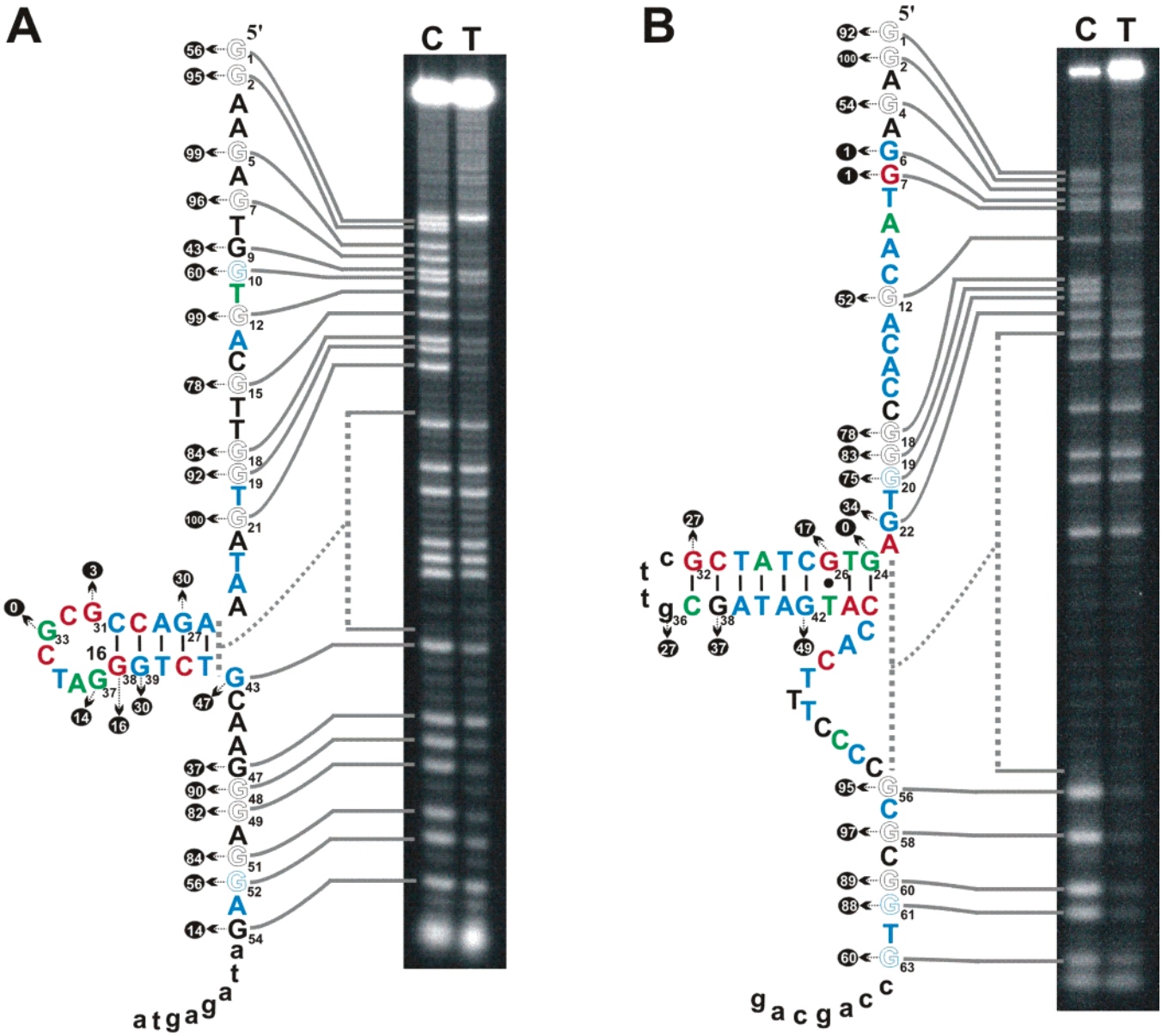

FIGURE 6: Methylation interference assays. 3′-Labeled DNAzyme constructs (extra noncatalytically essential nucleotides shown in lowercase) were treated with DMS either before (Test-T) or after (Control-C) a self-phosphorylation reaction was performed. Under our reaction condition, DMS methylated the N7 position of one guanine per deoxyribozyme molecule. Methylated guanines were cleaved by piperidine and cleaved fragments were resolved by a denaturing 10% PAGE gel. Methylated guanines that disrupt deoxyribozyme activity appear lighter in lane T than lane C. The degree of interference at each guanine was normalized as described in Materials and Methods, with 0 being the least observable interference and 100 being the most. Positions that scored above 50 are indicated by outlined text.

vented labeling the constructs on their 5′ ends, so each construct was 3′-radiolabeled using a primer extension protocol. The 3′-end of each minimized construct was also extended to introduce several wild-type but noncatalytically essential nucleotides (lowercase letters in Figure 6) so that the shortest piperidine cleavage fragment was large enough to be observed on a PAGE gel. Addition of the extra sequence had no substantial effect on the catalytic rate of either DNAzyme (data not shown). Methylated guanines that hindered proper enzymatic activity were identified by their absence in the resultant ladder (T lanes in Figure 6) as compared to a control lane where all guanines are represented (C lane in Figure 6). Since the DNAzyme constructs were labeled at the 3′-end, the autoradiogram is read from top to bottom in the 5′ to 3′ direction. The degree of interference was calculated using densitometry measurements of corresponding bands from each lane with a value of 100 indicating the most interference observed to 0 indicating the least. These values are given in the blue circles shown next to their corresponding guanines within Figure 6. In both DNAzyme constructs, bases with values above 50 were considered to yield a substantial interference effect and were represented as outlined in the text within Figure 6.

The methylation of the N7 position of guanine should have no effect on standard duplexes and unstructured loops. As expected, there is no substantial methylation interference occurring at the guanines of the confirmed stem-loop of Dk1 and Dk2. On the other hand, methylation of the conserved guanines (in black) in both deoxyribozymes creates severe interference effects. The exceptions are G9, G47, and G54 of Dk1 as less substantial interference was observed at these positions. Another exception was G38, a conserved base in

Dk2. However, this position is located in Stem-1 of Dk2 and has also been proven unnecessary by the covariation experiments described in Figure 5.

It can be surmised from the number of guanines for which methylation effects are observed (indicated as outlined letters in Figure 6) that there are substantial tertiary interactions involving both conserved and nonconserved guanines within these deoxyribozymes. Interference effects were observed at guanines located within the putative Stem-3 and Stem-4 regions of Dk2 (Figure 5), such as G18−20. These data cannot be used to rule out the formation of these small helical structures. However, if those helices are real, there is another level of critical tertiary contacts involving some of the guanines in these elements. The existence of putative Stem-2 of Dk2 was consistent with the mutation data (Figure 5). However, G61 and G63 within this stem also displayed considerable methylation interference. This, along with the observation that these two nucleotides were not absolutely conserved from the reselection data (Figure 2B), suggests that these two nucleotides may be intimately surrounded by structurally important nucleotides in the tertiary folding of the deoxyribozyme.

DISCUSSION

From the data presented above, it is apparent that both Dk1 and Dk2 have a common global structure arrangement that features a centrally located stem-loop element and a structural domain of higher-order tertiary interactions composed of two highly conserved stretches of nucleotides. The stem-loop element does not play a catalytic role, on the basis of the results from the loop truncation and stem-changing experiments. The observation that reduction of the length of the stem in the trans constructs of each deoxyribozyme resulted in loss of catalytic activity suggests that the tertiary interactions resulting from the two single-stranded stretches of nucleotides are not strong enough to hold the deoxyribozyme structure together. From this analysis, we conclude that the stem-loop element in each deoxyribozyme acts as an anchor for the formation of the complex tertiary structure by the rest of the deoxyribozyme.

As the stem-loop element appears to play a noncatalytic role, the nonhelical regions of Dk1 or Dk2 must be responsible for binding ATP or GTP and orientating the 5′-hydroxyl of the deoxyribozyme in a proper position to facilitate phosphoryl transfer. On the basis of the ATP requirement of Dk1, this portion of the sequence may contain a variant of the well-studied anti-ATP (ATP-binding) DNA aptamer. Although sequence analysis does not reveal a complete ATP-binding DNA aptamer sequence residing in Dk1, finding a variant of the aptamer within this ATP-dependent DNAzyme would not be surprising. Lorsch and Szostak used the anti-ATP RNA aptamer as a scaffold to isolate the first self-phosphorylating ribozyme (*35*). Originally, the anti-ATP DNA aptamer was thought to be composed of a nonhelical G-quartet system (*36*). However, this aptamer was later found, through NMR experiments, to adopt a largely helical structure containing two sheared G−G base pairs and two G−A mismatches with a widened minor groove binding pocket able to bind two ATP molecules (*37*). The nonhelical regions flanking the stem-loop of Dk1 may be analogous in overall structure to the ATP-binding DNA aptamer. The hydrogen bonds within a sheared G−G base pair do involve the N7 position of guanine; thus, this hypothesis has not been ruled out by our experimental data. Since Dk2 selectively utilizes GTP, it too by definition must contain a GTP-binding aptamer within its structure. However, to date there have been no published GTP-binding DNA aptamers with which to perform a sequence comparison.

There are precedents for non-Watson−Crick dominated structures within other DNAzymes. A DNA-cleaving deoxyribozyme has been shown to recognize its substrate through duplex and triplex interactions (*12*). Triplex interactions such as those observed for the DNA-cleaving deoxyribozyme are a possibility since G*G−C triplex interactions require the N7 position of central guanine to act as a hydrogen bond donor. In addition, G-quadruplex structures have been proposed in several DNAzymes. A Ca^{2+}-dependent self-phosphorylating DNAzyme (*13*), the Class I self-adenylating DNAzyme (*15*), a metallase DNAzyme (*38*), and a recently isolated thymine dimer cleaving deoxyribozyme (*39*) are all proposed to have structures based upon a stack of two to four G-quartets. The G-rich nature of Dk1 and Dk2 (43% for Dk1; 33% for Dk2), and the abundance of potassium in the buffer used in their selection, hints at a tertiary structure based on G-quartets. However, the existence of a G-quartet structure within Dk1 or Dk2 is not supported by monovalent ion-dependence tests that demonstrated both Dk1 and Dk2 could function in the absence of potassium (unpublished results). In addition, the methylation interference patterns of both Dk1 and Dk2 do not reflect an easily discernible G-quartet system. For one to be present in either structure, it would have to be highly altered.

The finding that both Dk1 and Dk2 have a stem-loop anchored tertiary structure has implications for future in vitro selection experiments. It may be advantageous to incorporate centrally located stem-loop element flanked by random regions in predesigned libraries when selecting deoxyribozymes that require interaction with small-molecule substrates, as in the case with Dk1 and Dk2. Invariable stem elements may add structural rigidity, as compared to fully randomized libraries, to promote association of the distal random regions of the library. Invariable stems would also dramatically increase the amount of searchable sequence space, allowing a more complete exploration of the structural possibilities within the random flanking regions. The concept of utilizing prestructured libraries has already been used in the successful selection of high-affinity GTP-binding RNA aptamers (*40*) and aspartame-recognition elements (*41*).

This study can serve as a foundation for future structural studies designed to investigate how these DNAzymes selectively recognize different substrates, and with the aid of divalent metal ion cofactors, bring about substantial rate enhancements. Several somewhat less proficient self-phosphorylating DNAzymes were also isolated from the in vitro selection experiments used to isolate both Dk1 and Dk2 (*14*). Most of these DNAzyme differ from Dk1 and Dk2 in their divalent metal ion requirements and substrate specificity. It will be interesting to see whether these seemingly unrelated sequences, which share catalytic function, rely on the same overall global structure observed for Dk1 and Dk2. Alternatively, structural investigation of this large family of self-phosphorylating deoxyribozymes may reveal the full potential of DNA to create structurally diverse catalysts.

SUPPORTING INFORMATION AVAILABLE

Sequences of isolated clones and first-order rate constants for various Dk1 and Dk2 constructs. This material is available free of charge via the Internet at http://pubs.acs.org.

REFERENCES

1. Breaker, R. R., and Joyce, G. F. (1994) A DNA enzyme that cleaves RNA, *Chem. Biol. 1*, 223−229.
2. Breaker, R. R., and Joyce, G. F. (1995) A DNA enzyme with Mg^{2+}-dependent RNA phosphoesterase activity, *Chem. Biol. 2*, 655−660.
3. Faulhammer, D., and Famulok, M. (1996) The Ca^{2+} ion as a cofactor for a novel RNA-cleaving deoxyribozyme., *Angew. Chem., Int. Ed. Engl. 35*, 2809−2813.
4. Santoro, S. W., and Joyce, G. F. (1997) A general purpose RNA-cleaving DNA enzyme, *Proc. Natl. Acad. Sci. U.S.A. 94*, 4262−4266.
5. Geyer, C. R., and Sen, D. (1997) Evidence for the metal-cofactor independence of an RNA phosphodiester-cleaving DNA enzyme, *Chem. Biol. 4*, 579−593.
6. Roth, A., and Breaker, R. R. (1998) An amino acid as a cofactor for a catalytic polynucleotide, *Proc. Natl. Acad. Sci. U.S.A. 95*, 6027−6031.
7. Li, J., Zheng, W., Kwon, A. H., and Lu, Y. (2000) In vitro selection and characterization of a highly efficient Zn(II)-dependent RNA-cleaving deoxyribozyme, *Nucleic Acids Res. 28*, 481−488.
8. Feldman, A. R., and Sen, D. (2001) A new and efficient DNA enzyme for the sequence-specific cleavage of RNA, *J. Mol. Biol. 313*, 283−294.
9. Lermer, L., Roupioz, Y., Ting, R., and Perrin, D. M. (2002) Toward an RNaseA Mimic: A DNAzyme with Imidazoles and Cationic Amines, *J. Am. Chem. Soc. 124*, 9960−9961.
10. Cruz, R. P. G., Withers, J. W., and Li, Y. (2004) Dinucleotide junction cleavage versatility of 8-17 deoxyribozyme, *Chem. Biol. 11*, 57−67.
11. Carmi, N., Shultz, L. A., and Breaker, R. R. (1996) In vitro selection of self-cleaving DNAs, *Chem. Biol. 3*, 1039−1046.
12. Carmi, N., Balkhi, S. R., and Breaker, R. R. (1998) Cleaving DNA with DNA, *Proc. Natl. Acad. Sci. U.S.A. 95*, 2233−2237.
13. Li, Y., and Breaker, R. R. (1999) Phosphorylating DNA with DNA, *Proc. Natl. Acad. Sci. U.S.A. 96*, 2746−2751.
14. Wang, W., Billen, L. P., and Li, Y. (2002) Sequence diversity, metal specificity, and catalytic proficiency of metal-dependent phosphorylating DNA enzymes, *Chem. Biol. 9*, 507−517.
15. Li, Y., Liu, Y., and Breaker, R. R. (2000) Capping DNA with DNA, *Biochemistry 39*, 3106−3114.
16. Cuenoud, B., and Szostak, J. W. (1995) A DNA metalloenzyme with DNA ligase activity, *Nature 375*, 611−614.
17. Levy, M., and Ellington, A. D. (2001) Selection of deoxyribozyme ligases that catalyze the formation of an unnatural internucleotide linkage, *Bioorg. Med. Chem. 9*, 2581−2587.
18. Sreedhara, A., Li, Y., and Breaker, R. R. (2004) Ligating DNA with DNA, *J. Am. Chem. Soc. 126*, 3454−3460.
19. Flynn-Charlebois, A., Prior, T. K., Hoadley, K. A., and Silverman, S. K. (2003) In vitro evolution of an RNA-cleaving DNA enzyme into an RNA ligase switches the selectivity from 3′-5′ to 2′-5′, *J. Am. Chem. Soc. 125*, 5346−5350.
20. Flynn-Charlebois, A., Wang, Y., Prior, T. K., Rashid, I., Hoadley, K. A., Coppins, R. L., Wolf, A. C., and Silverman, S. K. (2003) Deoxyribozymes with 2′-5′ RNA ligase activity, *J. Am. Chem. Soc. 125*, 2444−2454.
21. Sheppard, T. L., Ordoukhanian, P., and Joyce, G. F. (2000) A DNA enzyme with N-glycosylase activity, *Proc. Natl. Acad. Sci. U.S.A. 97*, 7802−7807.
22. Li, Y., and Sen, D. (1996) A catalytic DNA for porphyrin metalation, *Nat. Struct. Biol. 3*, 743−747.
23. Mei, S. H., Liu, Z., Brennan, J. D., and Li, Y. (2003) An efficient RNA-cleaving DNA enzyme that synchronizes catalysis with fluorescence signaling, *J. Am. Chem. Soc. 125*, 412−420.
24. Liu, Z., Mei, S. H., Brennan, J. D., and Li, Y. (2003) Assemblage of signaling DNA enzymes with intriguing metal-ion specificities and pH dependences, *J. Am. Chem. Soc. 125*, 7539−7545.
25. Li, J., and Lu, Y. (2000) A Highly Sensitive and Selective Catalytic DNA Biosensor for Lead Ions, *J. Am. Chem. Soc. 122*, 10466−10467.
26. Stojanovic, M. N., de Prada, P., and Landry, D. W. (2000) Homogeneous assays based on deoxyribozyme catalysis, *Nucleic Acids Res. 28*, 2915−2918.
27. Stojanovic, M. N., and Stefanovic, D. (2003) Deoxyribozyme-based half-adder, *J. Am. Chem. Soc. 125*, 6673−6676.
28. Wang, Y., and Silverman, S. K. (2003) Deoxyribozymes that synthesize branched and lariat RNA, *J. Am. Chem. Soc. 125*, 6880−6881.
29. Silverman, S. K. (2004) Breaking Up is Easy to Do (If You're a DNA Enzyme that Cleaves RNA), *Chem. Biol. 11*, 7−8.
30. Cate, J. H., Gooding, A. R., Podell, E., Zhou, K., Golden, B. L., Kundrot, C. E., Cech, T. R., and Doudna, J. A. (1996) Crystal structure of a group I ribozyme domain: principles of RNA packing, *Science 273*, 1678−1685.
31. Ferre-D'Amare, A. R., Zhou, K., and Doudna, J. A. (1998) Crystal structure of a hepatitis delta virus ribozyme, *Nature 395*, 567−574.
32. Rupert, P. B., and Ferre-D'Amare, A. R. (2001) Crystal structure of a hairpin ribozyme-inhibitor complex with implications for catalysis, *Nature 410*, 780−786.
33. Chiuman, W., and Li, Y. (2002) Making AppDNA using T4 DNA ligase, *Bioorg. Chem. 30*, 332−349.
34. Zuker, M. (2003) Mfold web server for nucleic acid folding and hybridization prediction, *Nucleic Acids Res. 31*, 3406−3415.
35. Lorsch, J. R., and Szostak, J. W. (1994) In vitro evolution of new ribozymes with polynucleotide kinase activity, *Nature 371*, 31−36.
36. Huizenga, D. E., and Szostak, J. W. (1995) A DNA aptamer that binds adenosine and ATP, *Biochemistry 34*, 656−665.
37. Lin, C. H., and Patel, D. J. (1997) Structural basis of DNA folding and recognition in an AMP-DNA aptamer complex: distinct architectures but common recognition motifs for DNA and RNA aptamers complexed to AMP, *Chem. Biol. 4*, 817−832.
38. Li, Y., and Sen, D. (1997) Toward an efficient DNAzyme, *Biochemistry 36*, 5589−5599.
39. Chinnapen, D. J., and Sen, D. (2004) A deoxyribozyme that harnesses light to repair thymine dimers in DNA, *Proc. Natl. Acad. Sci. U.S.A. 101*, 65−69.
40. Davis, J. H., and Szostak, J. W. (2002) Isolation of high-affinity GTP aptamers from partially structured RNA libraries, *Proc. Natl. Acad. Sci. U.S.A. 99*, 11616−11621.
41. Ferguson, A., Boomer, R. M., Kurz, M., Keene, S. C., Diener, J. L., Keefe, A. D., Wilson, C., and Cload, S. T. (2004) A novel strategy for selection of allosteric ribozymes yields Ribo-Reporter™ sensors for caffeine and aspartame, *Nucleic Acids Res. 32*, 1756−1766.

BI0483054